

SANDIA REPORT

SAND2006-7100

Unlimited Release

Printed November 2006

RF/Microwave Properties and Applications of Directly Assembled Nanotubes and Nanowires: LDRD Project 102662 Final Report

Mark Lee, Eric A. Shaner, Clark Highstrete, Albert A. Talin, Frank E. Jones,
Aaron Vallett, and Theresa Mayer

Prepared by
Sandia National Laboratories
Albuquerque, New Mexico 87185 and Livermore, California 94550

Sandia is a multiprogram laboratory operated by Sandia Corporation,
a Lockheed Martin Company, for the United States Department of Energy's
National Nuclear Security Administration under Contract DE-AC04-94AL85000.

Approved for public release; further dissemination unlimited.



Issued by Sandia National Laboratories, operated for the United States Department of Energy by Sandia Corporation.

NOTICE: This report was prepared as an account of work sponsored by an agency of the United States Government. Neither the United States Government, nor any agency thereof, nor any of their employees, nor any of their contractors, subcontractors, or their employees, make any warranty, express or implied, or assume any legal liability or responsibility for the accuracy, completeness, or usefulness of any information, apparatus, product, or process disclosed, or represent that its use would not infringe privately owned rights. Reference herein to any specific commercial product, process, or service by trade name, trademark, manufacturer, or otherwise, does not necessarily constitute or imply its endorsement, recommendation, or favoring by the United States Government, any agency thereof, or any of their contractors or subcontractors. The views and opinions expressed herein do not necessarily state or reflect those of the United States Government, any agency thereof, or any of their contractors.

Printed in the United States of America. This report has been reproduced directly from the best available copy.

Available to DOE and DOE contractors from
U.S. Department of Energy
Office of Scientific and Technical Information
P.O. Box 62
Oak Ridge, TN 37831

Telephone: (865) 576-8401
Facsimile: (865) 576-5728
E-Mail: reports@adonis.osti.gov
Online ordering: <http://www.osti.gov/bridge>

Available to the public from
U.S. Department of Commerce
National Technical Information Service
5285 Port Royal Rd.
Springfield, VA 22161

Telephone: (800) 553-6847
Facsimile: (703) 605-6900
E-Mail: orders@ntis.fedworld.gov
Online order: <http://www.ntis.gov/help/ordermethods.asp?loc=7-4-0#online>



SAND 2006-7100
Unlimited Release
Printed November 2006

**RF/Microwave Properties and Applications of Directly
Assembled Nanotubes and Nanowires: LDRD Project 102662
Final Report**

Mark Lee, Eric A. Shaner, and Clark Highstrete
Semiconductor Materials and Device Sciences Department

Sandia National Laboratories
P.O. Box 5800
Albuquerque, NM 87185-1415

A. Alec Talin and Frank E. Jones
Nanoscale Science and Technology Department

Sandia National Laboratories
P.O. Box 969
Livermore, CA 94550-0969

Aaron Vallett and Theresa Mayer
Dept. of Electrical Engineering
The Pennsylvania State University
University Park, PA 16802

Abstract

LDRD Project 102662 provided support to pursue experiments aimed at measuring the basic electrodynamic response and possible applications of carbon nanotubes and silicon nanowires at radiofrequency to microwave frequencies, approximately 0.01 to 50 GHz. Under this project, a method was developed to integrate these nanomaterials onto high-frequency compatible co-planar waveguides. The complex reflection and transmission coefficients of the nanomaterials was studied as a function of frequency. From these data, the high-frequency loss characteristics of the nanomaterials were deduced. These data are useful to predict frequency dependence and power dissipation characteristics in new rf/microwave devices incorporating new nanomaterials.

Contents

1. Introduction	7
2. Nanomaterial assembly and measurement	8
3. Nanomaterial high-frequency loss characterization	12
4. References	15

1. Introduction

Carbon nanotubes (CNTs) and silicon nanowires (SiNWs) are predicted to have unique and desirable high-frequency characteristics [1] that can lead to potentially disruptive advancements in radiofrequency and microwave technologies for very high-speed electronics and chemical/biological sensing. While there exists extensive efforts to characterize and exploit DC electrical properties of such nanomaterials, [2] even the most fundamental rf/microwave properties of CNTs and SiNWs remain nearly unexplored and certainly undeveloped. One of the major upcoming frontiers in nanomaterial research will be in high-frequency properties and applications. To open this frontier will require a focused effort to measure and model accurately the basic electrodynamic response of CNTs and SiNWs across the range of frequencies relevant to high-speed communication, computation, radar, *etc.* (*i.e.*, MHz up to tens of GHz). Once the electrodynamic physics is better understood, a number of innovative applications can be envisioned. For example, pure nanowires and nanotubes are believed to exhibit ballistic charge transport, [3] a phenomenon that does not exist in micro- or macroscopic materials. This novel transport mechanism could be exploited to construct a new class of extremely power-efficient, frequency-agile rf/microwave oscillators [4] and detectors. [5]

Before being able to engineer high-frequency devices using CNTs and SiNWs, it is necessary to know and understand their electrodynamic characteristics. Such knowledge has proven difficult to obtain, and only now are rudimentary empirical results being reported. [6,7,8,9] Measurement of high-frequency properties of CNTs and SiNWs presents a significant challenge since it is not obvious how to integrate such materials into a broadband microwave compatible measurement. The need to precisely place nanomaterials in a high-frequency waveguide circuit requires small electrode spacing dimensions not easily compatible with the need to make the waveguide impedance near 50Ω and low-loss. Our solution is to use dielectrophoresis directed assembly methods to place nanomaterials across the gaps of co-planar waveguide (CPW) electrodes. The nanotubes/wires are thus aligned so as to be maximally polarized by the propagating electric field. This is a *contactless* measurement; the nanomaterial couples capacitively to the propagating electric field of the CPW. These measurements thus yield the intrinsic AC conductivity of the nanomaterials without the complication of electrical contacts.

This information will generate the input needed to begin engineering high-frequency devices incorporating these nanomaterials.

2. Nanomaterial assembly and measurement

While there have been extensive efforts to examine and understand the DC electrical properties of carbon nanotubes, the high frequency (AC) response of these nanomaterials has only recently begun to receive experimental attention. Short (*i.e.*, few microns long), high purity single-wall carbon nanotubes (SWCNTs) and silicon nanowires (SiNWs) may have unusual and conceivably very useful AC properties at microwave to millimeter-wave frequencies. Attractive high-frequency properties and applications of SWCNTs that have been studied theoretically or numerically include: very small parasitic capacitance, [10] unusual AC response from Luttinger liquid physics associated with high-mobility one-dimensional conductors, [11] and various unconventional electronic properties. [5,12] Recently, radio-frequency and microwave experiments studying rectification and conductance on transistors [6,8,9,13] and diodes [10,14] as well as measurements of linear impedance to 8 MHz, [15] have been reported on devices formed from either individual or a small number of SWCNTs.

A major concern in many of these studies has been the intrinsic high-frequency power dissipation of SWCNTs. Interestingly, the transistor-related works have generally concluded that either AC loss is below measurement resolution or, if AC dissipation exists at all, it is nearly frequency-independent and hence is not the limiting factor in determining device bandwidth. In these works, empirically measured loss and bandwidth have been reported to be set by relatively large instrumental and device parasitic roll-offs and by systematic measurement variations. On the other hand, direct measurement of frequency-dependent microwave loss in dense mixtures of double-wall CNTs has recently been reported. [16] It remains unclear whether SWCNTs are intrinsically lossless at room temperature or whether any AC dissipation in SWCNTs is simply below the resolution of the experiments reported to date.

Here we report quantitative measurements of the reflection and transmission scattering coefficients (*S*-parameters) in SWCNTs and SiNWs from 0.01 to 50 GHz. To obtain higher signal and improve reproducibility, arrays consisting of order 10^3

nanotubes/wires were measured, so that the response is from small ensembles of rather than from a single nanotube or wire. Good signal-to-noise ratio and a very high level of systematic reproducibility were achieved. Most significantly, in all samples measured the *S*-parameters indicate a high-frequency power dissipation that can be directly attributed to the nanomaterial arrays.

SWCNT material was purchased from SES Research, while a set of SiNWs with different dopant types and densities were grown by laser ablation at Penn State. These nanomaterials were separated and put into suspension, and then directly assembled onto broadband co-planar waveguides (CPWs) using AC dielectrophoresis (ACDEP), [17,18] as illustrated in the insets of Fig. 1. The SiNWs were suspended in ethanol. To control for possible influence of surfactants on the SWCNTs, two suspensions were used. One, described in detail in Ref. 14, used single-stranded DNA as a surfactant in an aqueous suspension. The second suspension was prepared by sonicating 5 mg/mL of SWCNT material, without surfactant, in dimethylformamide (DMF). Typical ACDEP parameters used were 10 V (peak-to-peak) assembly voltage at 10 MHz, 30 s time, 1 μ L suspension volume, and 2 μ m electrode gap. No attempt was made to isolate systematically the effect of any one parameter on the assembled nanomaterial array characteristics.

The ACDEP process preferentially assembles metallic nanotubes and wires, as opposed to semiconducting ones. [17] The SWCNTs and SiNWs were assembled across the CPW gaps between center conductor and ground planes so as to be aligned with the electric field polarization of the propagating mode in the CPW, maximizing interaction between nanomaterial and the electromagnetic field (see Fig. 1 insets). A previous study [18] of SWCNT transistors fabricated using very similar ACDEP conditions showed that roughly 1/5 of the devices exhibited semiconducting characteristics, with the rest metallic. No post-deposition annealing was done. Electron micrographs showed the ACDEP resulted in fairly regular arrays (Fig 1(b) inset) over a 1 to 2 mm span along the CPW. The SWCNTs had nanotube ropes mixed in with single tubes. The SWCNT suspension using DNA surfactant usually resulted in fewer ropes compared to the DMF suspension and so was used more than the DMF suspension.

The CPWs consisted of 20 nm Ti and 200 nm Au evaporated on 0.5 mm thick fused quartz substrates. In some cases, 100 nm of silicon nitride was deposited onto the Au

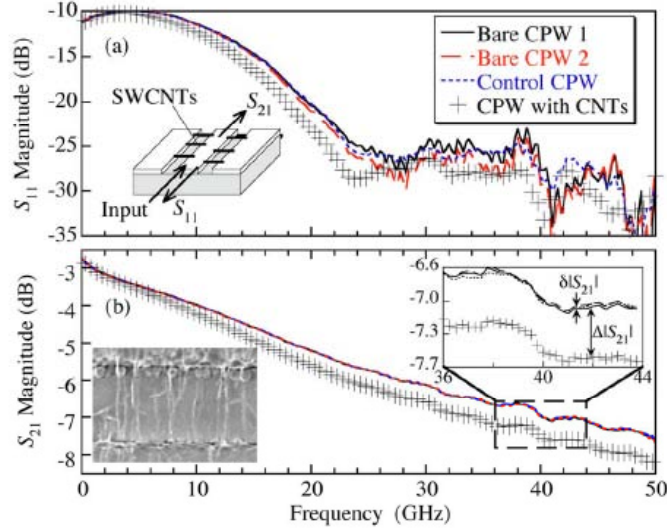


FIG. 1. (a) $|S_{11}|$ and (b) $|S_{21}|$ vs. frequency for two separate CPWs of same design. “Bare” indicates the CPWs before ACDEP. “Control CPW” is CPW 2 after ACDEP but without nanotubes. The “+” data are for CPW 1 after ACDEP with nanotubes. Insets: (a) Schematic of the measurement geometry. (b) Lower: Electron microscope image of SWCNTs assembled across a 1 μm wide gap between center conductor and one ground plane of a CPW. Upper: Expanded view of the $|S_{21}|$ data from 36 to 44 GHz. The measurement uncertainty $\delta|S_{21}|$ and the signal magnitude $\Delta|S_{21}|$ from the SWCNT array are indicated.

surface to prevent DC electrical contact between nanotubes/wires and the CPW electrodes. Microwave loss from assembled nanomaterial arrays was always observed in these insulated samples as well as in samples where the nanotubes/wires were in physical contact (but not annealed) with the Au, so contact resistance can be ruled out as the source of microwave dissipation. CPW gap sizes used were 1, 2, and 3 μm , and lengths of 1 and 2 mm. The characteristic impedance of the bare CPWs (*i.e.*, without SWCNTs) was designed for 50 Ω across as broad a band as possible.

Measurements were made using a network analyzer calibrated at room temperature with a commercial short-open-load-through off-wafer standard. The measurement system was calibrated to 50 Ω impedance within 1% tolerance across the 0.01 to 50 GHz band. The magnitudes of the scattering or S -parameters S_{ij} ($i, j = 1, 2$) were recorded as a function of frequency (see Fig. 1(a) inset). The CPWs were symmetric between input and output, so the voltage reflection amplitude $S_{11} = S_{22}$ and transmission amplitude $S_{21} = S_{12}$. Experimental procedure was as follows: S -parameters were first measured for each

bare CPW. SWCNTs or SiNWs were then assembled on the CPWs and the S -parameters were re-measured. In every batch of samples undergoing the ACDEP process, at least one CPW was processed alongside but without nanomaterial. These CPWs are experimental controls used to monitor possible spurious processing effects and systematic measurement reproducibility. Thus the *changes* in S_{11} and S_{21} between the CPWs with SWCNTs or SiNWs and the control CPWs isolate the contribution of the SWCNT arrays from imperfections in real CPW characteristics. To have confidence that changes in the S -parameters are due to the SWCNTs or SiNWs, a very high level of systematic measurement reproducibility is required to eliminate measurement-to-measurement variations.

Fig. 1 demonstrates the degree of reproducibility in a SWCNT array. Fig 1(a) plots $|S_{11}|$ and Fig. 1(b) plots $|S_{21}|$ vs. frequency for two separate CPWs of same design. The $|S_{11}|$ curves for bare CPW 1 and bare CPW 2 overlap strongly. The large structure in the bare $|S_{11}|$ data result from frequency-dependent variations of the CPW impedance. Reproducible fine structure are characteristics of this particular CPW design and its interface with the microwave probes. Random noise is seen when $|S_{11}| < -25$ dB. The bare CPWs' $|S_{21}|$ curves are nearly indistinguishable. The general decrease with increasing frequency in the bare $|S_{21}|$ is attributable to surface resistance in the Au electrodes. In general, CPWs of the same design gave quantitatively reproducible S -parameter characteristics.

Bare CPW 1 and bare CPW 2 then underwent ACDEP with CPW 2 as control (no nanotubes) and a SWCNT array assembled on CPW 1. The post-ACDEP S -parameters are also shown in Fig. 1. The control CPW is indistinguishable from the bare CPWs. This demonstrates that the ACDEP procedure does not significantly affect the S -parameters and that the measurement technique has a very high degree of systematic reproducibility. By contrast, the S -parameters of CPW 1 with a SWCNT array assembled are clearly different from the bare and control CPWs.

Of primary importance is the systematic measurement uncertainty, $\delta|S_{ij}|$, on the bare and control CPWs. This uncertainty is graphically represented by the spread among the bare and control CPW S -parameter curves in Fig. 1. For example, $\delta|S_{21}|$ is indicated in the inset of Fig. 1(b). Looking at the S -parameters of the CPW assembled with a

SWCNT array, the signal magnitude attributable to the SWCNTs is the *difference*, $\Delta|S_{ij}| = |S_{ij}|(\text{with SWCNTs}) - |S_{ij}|(\text{control CPW})$, as indicated graphically for $\Delta|S_{21}|$ in Fig. 1(b) inset. The relevant signal-to-noise is the ratio $\Delta|S_{ij}|/\delta|S_{ij}|$. For $|S_{21}|$ this ratio was typically between 10 to 20 dB, whereas for $|S_{11}|$ the signal-to-noise was between 5 to 10 dB, falling to 0 dB when $|S_{11}| < -25$ dB, where random noise dominates.

3. Nanomaterial high-frequency loss characterization

The microwave power dissipation, as a fraction of input power, in a symmetric impedance-matched waveguide is $P_{\text{loss}} = 1 - (|S_{11}|^2 + |S_{21}|^2)$, where a positive number means power lost from the propagating wave. Excess power dissipation, *i.e.*, above that of the bare CPW, contributed by SWCNT or SiNW arrays is $\Delta P_{\text{loss}} = P_{\text{loss}}(\text{with nanomaterial array}) - P_{\text{loss}}(\text{bare CPW})$, which is plotted in Fig. 2 for four different SWCNT samples on CPWs with 2 μm gaps and 2 mm long interaction lengths. SWCNT arrays in samples A and C had DNA surfactant while samples B and D had no surfactant, but the ACDEP parameters used were different for all four. The data of Fig. 2 represent well the 1 to 10% range of power dissipation observed in over 60 different samples with SWCNT arrays assembled under a variety of conditions and having different total number and number density of nanotubes. No clear trend in dissipation magnitude variation was noticed between SWCNT arrays with DNA surfactant and arrays without

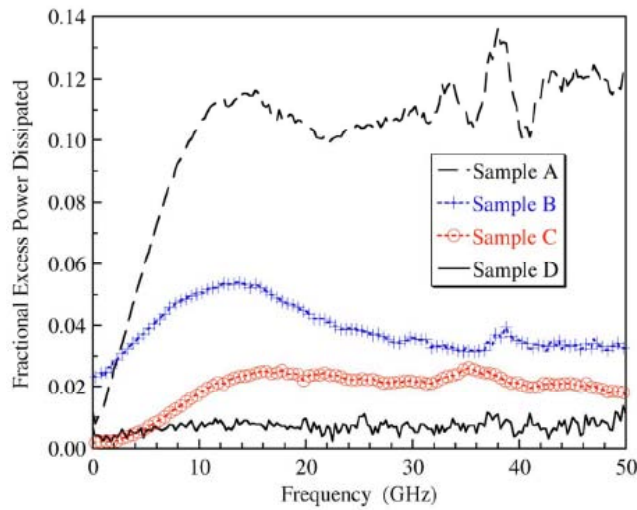


FIG. 2. Excess fractional power dissipation after assembly of SWCNT arrays, relative to the loss of the bare or control CPW. Sample C's raw data are shown in Fig. 1.

surfactant, so the DNA surfactant is unlikely to contribute significantly to the microwave loss. Regardless of sample preparation, the important point is that in all samples measured, more power was dissipated after assembly of the SWCNT arrays than on the corresponding bare or control CPWs. The sample with the largest excess loss showed a $\sim 10\%$ increase in loss (near 20 GHz) attributable to the SWCNT array. This array was comprised of roughly 10^3 SWCNTs. If the loss is naively divided among the SWCNTs, the average *individual* SWCNT would contribute $\sim 0.01\%$ more loss to that of the bare CPW. That small a loss is well below our experimental resolution, so this experiment would be unable to observe the AC dissipation from a single or small number of SWCNTs. Thus the results reported here are not necessarily inconsistent with Refs. 6, 8, and 9.

It is of physical interest to derive a loss coefficient for the SWCNT arrays. The power dissipated in a waveguide of length L at frequency f is expressed as $P_{\text{loss}} = 1 - \exp(-\alpha(f)L)$, where $\alpha(f)$ is the attenuation coefficient. To derive the loss properties of the SWCNTs and SiNWs, we write $\alpha = \alpha_0 + \alpha_{\text{NANO}}$, where α_0 is the attenuation of the bare or control waveguide and α_{NANO} is the additional loss after assembling a SWCNT or SiNW array. Using the data like that shown Fig. 2, the magnitude and frequency dependence of α_{CNT} derived for these samples is shown in Fig. 3. α_{CNT} for these samples

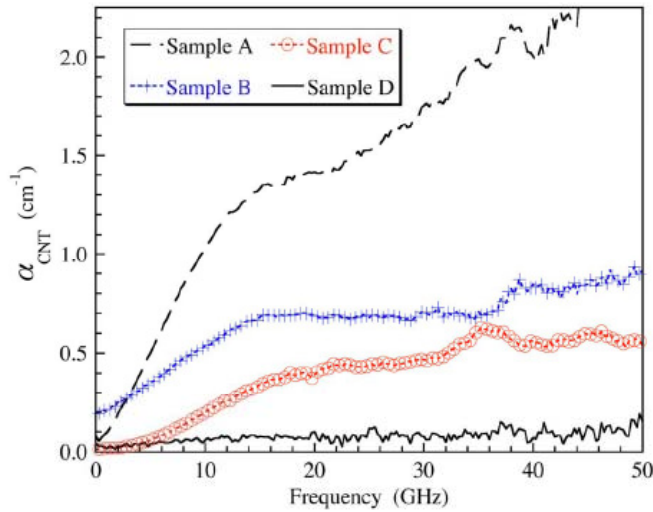


FIG. 3. Frequency dependence of the attenuation coefficient α_{CNT} of the SWCNT arrays on the four samples whose raw power loss data is shown in Fig. 2.

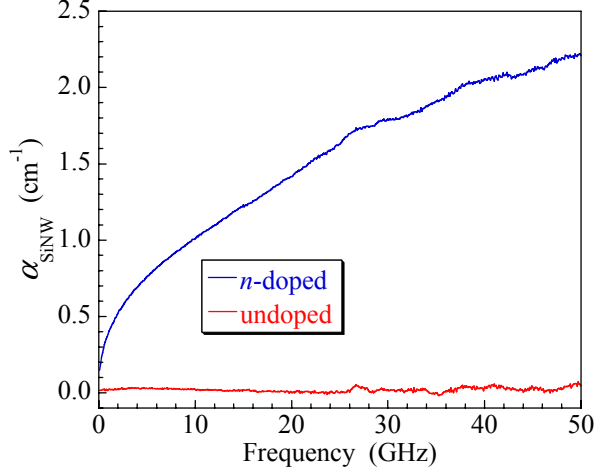


FIG. 4. Frequency dependence of the loss coefficient α_{SiNW} for n -doped and undoped SiNW arrays, taken using measurement procedures identical to those used for SWCNT arrays. The undoped sample has loss coefficient below measurement resolution.

have very different magnitudes and the data shown reflect the range of α_{CNT} values derived across all samples measured. Interestingly, however, apart from magnitude, the functional forms of the frequency dependencies measured are roughly similar across different samples. α_{CNT} is generally observed to increase with increasing frequency, with a roughly linear frequency dependence at relatively low frequencies, *i.e.*, below ~ 10 GHz. This linear dependence is qualitatively similar to the low-frequency loss behavior reported in Ref. 16.

In heavily doped n -type SiNWs, a positive loss coefficient α_{SiNW} is also always observed, as shown in Fig. 4. The frequency dependence of α_{SiNW} shows a much more square-root shape which is characteristic of skin-depth power loss in a metal, in contrast to the frequency dependence of α_{CNT} . However, the estimated skin depth of these SiNWs at the upper 50 GHz frequency limit is significantly larger than the ~ 100 nm diameter of the SiNWs, so in principal the classic metal skin-depth frequency dependence should not be applicable here. The undoped SiNW arrays show a loss coefficient that is below our measurement resolution. It is unknown at this time whether this indicates a lossless high-frequency conduction mechanism or whether the loss is simply very small.

4. References

- [1] F. Léonard and J. Tersoff, Phys. Rev. Lett. **85**, 4567 (2000)
- [2] See for example: I. Kratochvilova, *et al.*, J. Mater. Chem. **12**, 2927 (2002); P. L. McEuen and J. Y. Park, MRS Bulletin **29**, 272 (2004)
- [3] M. Bockrath, *et al.*, Nature **397**, 598 (1999); D. Mann, *et al.*, Nano Lett. **3**, 1541 (2003)
- [4] F. Léonard and J. Tersoff, Phys. Rev. Lett. **88**, 258302 (2002)
- [5] F. Léonard and J. Tersoff, Phys. Rev. Lett. **84**, 4693 (2000)
- [6] J. Appenzeller and D. J. Frank, Appl. Phys. Lett. **84**, 1771 (2004)
- [7] J. Kin, *et al.*, Phys. Rev. B **70**, 153402 (2004)
- [8] S. Rosenblatt, *et al.*, Appl. Phys. Lett. **87**, 153111 (2005)
- [9] Z. Yu and P. J. Burke, Nano Lett. **5**, 1403 (2005)
- [10] H. M. Manohara, *et al.*, Nano Lett. **5**, 1469 (2005)
- [11] P. J. Burke, IEEE Trans. Nanotech. **1**, 129 (2002)
- [12] G. Y. Slepyan, *et al.*, Phys. Rev. B **60**, 17136 (1999).
- [13] M. Zhang, *et al.*, Appl. Phys. Lett. **88**, 163109 (2006)
- [14] D. V. Singh, K. A. Jenkins, and J. Appenzeller, Elec. Lett. **41**, 280 (2005)
- [15] Y.-P. Zhao, *et al.*, Phys. Rev. B **64**, 201402R (2001)
- [16] M. Dragoman, *et al.*, Appl. Phys. Lett. **88**, 153108 (2006)
- [17] R. Krupke, F. Hennrich, H. v. Löhneysen, and M. M. Kappes, Science **301**, 344 (2003)
- [18] A. A. Talin, *et al.*, J. Vac. Sci. Technol. B **22**, 3107 (2004)

Distribution

1	MS 0123	LDRD Office, 1030
1	MS 1086	D. L. Barton, 1123
1	MS 1086	1123 Department File
5	MS 1415	M. Lee, 1123
1	MS 1415	C. Highstrete, 1123
1	MS 1415	E. A. Shaner, 1123
1	MS 1415	J. C. Barbour, 1120
1	MS 1415	R. Q. Hwang, 1110
1	MS 1427	J. M. Phillips, 1100
1	MS 9161	J. L. Lee, 8759
1	MS 9161	A. E. Pontau, 8750
1	MS 9401	A. A. Talin, 8759
1	MS 9401	F. E. Jones, 8759
1	MS 9405	R. W. Carling, 8700
1	MS 0161	Patent and Licensing Office, 1150
2	MS 0899	Technical Library, 4536
2	MS 9018	Central Technical Files, 8944